

ORIGINAL ARTICLE

Loss of PKC δ results in characteristics of Sjögren's syndrome including salivary gland dysfunction

GP Banninger¹, S Cha², MS Said², KM Pauley², CJ Carter¹, M Onate², BA Pauley², SM Anderson², ME Reyland¹

¹Department of Craniofacial Biology, School of Dental Medicine, University of Colorado, Anschutz Medical Campus, Aurora, CO;

²Department of Oral and Maxillofacial Diagnostic Sciences, College of Dentistry, University of Florida, Gainesville, FL, USA

OBJECTIVES: Chronic infiltration of lymphocytes into the salivary and lacrimal glands of patients with Sjögren's Syndrome (SS) leads to destruction of acinar cells and loss of exocrine function. Protein kinase C-delta (PKC δ) is known to play a critical role in B-cell maintenance. Mice in which the PKC δ gene has been disrupted have a loss of B-cell tolerance, multiple organ lymphocytic infiltration, and altered apoptosis. To determine whether PKC δ contributes to the pathogenesis of SS, we quantified changes in indicators of SS in PKC δ -/- mice as a function of age. Salivary gland histology, function, the presence of autoantibodies, and cytokine expression were examined.

MATERIALS AND METHODS: Submandibular glands were examined for the presence of lymphocytic infiltrates, and the type of infiltrating lymphocyte and cytokine deposition was evaluated by immunohistochemistry. Serum samples were tested by autoantibody screening, which was graded by its staining pattern and intensity. Salivary gland function was determined by saliva collection at various ages.

RESULTS: PKC δ -/- mice have reduced salivary gland function, B220+ B-cell infiltration, anti-nuclear antibody production, and elevated IFN- γ in the salivary glands as compared to PKC δ +/- littermates.

CONCLUSIONS: PKC δ -/- mice have exocrine gland tissue damage indicative of a SS-like phenotype.

Oral Diseases (2011) 17, 601–609

Keywords: PKC δ ; autoimmunity; Sjögren's syndrome

Introduction

Sjögren's syndrome (SS) is a chronic, autoimmune disorder marked by lymphocytic infiltration of exocrine glands, particularly the salivary and lacrimal glands (Fox and Kang, 1992). Destruction of acinar cells and the loss of exocrine function lead to the development of dry eyes (keratoconjunctivitis sicca) and dry mouth (xerostomia) (Kroneld *et al*, 1997; Humphreys-Beher *et al*, 1999). SS affects 0.5% of the population; however, women are affected at a rate eight times that of men (Bowman *et al*, 2004). The disease can occur as a primary disease, or secondary to other autoimmune disorders such as scleroderma, rheumatoid arthritis, or systemic lupus erythematosus (Bowman *et al*, 2004). The pathogenesis of SS is poorly understood, although most studies suggest that immune-mediated damage to the exocrine glands underlie the functional deficiencies seen. Animal models have been developed to study the pathogenesis of the disease; however, many fail to produce the persistent lesions and functional loss seen in human patients (Jonsson *et al*, 2007).

T-cell-mediated autoimmune responses have been observed to be central to the pathogenesis of SS, and in many spontaneous mouse models of SS CD4⁺, T cells predominate in the salivary gland infiltrates (Soyfoo *et al*, 2007). However, recent studies have suggested that functionally impaired B cells and alterations in apoptosis may also play an important role in the pathogenesis of SS (Youinou *et al*, 2007). Evidence of a dominant role of B cells in the genesis of SS includes the loss of immune tolerance, systemic antibodies to self-antigens, and accumulation of memory-type B cells in the inflamed parotid glands of human patients (Stott *et al*, 1998). Patients with SS may also have an increased circulation of B-cell-activating factor (BAFF) (7). Interestingly, transgenic mice that overexpress BAFF have an excess of mature B cells and a propensity to develop certain autoimmune diseases, including a SS-like syndrome that results in increased B-cell infiltration into the salivary glands, along

with salivary hypofunction (Ware, 2000; Groom *et al*, 2002). Destruction of circulating B cells in human patients with the anti-CD20 antibody, Rituximab, leads to the improvement of primary SS (Devauchelle-Pensec *et al*, 2007), supporting a crucial role for B cells in the pathogenesis of SS-like autoimmune disease (Khare *et al*, 2000).

Protein kinase C-delta (PKC δ) is a ubiquitously expressed member of the novel subfamily of PKC isoforms (Nishizuka, 1992) that is known to be critical for apoptosis (Reyland, 2009). Mice deficient for PKC δ (δ KO) have defects in apoptosis, particularly in response to genotoxic agents (Humphries, 2006, Allen-Petersen, 2010). Notably, δ KO mice develop systemic autoimmune disease associated with hyperproliferation of B220+ B cells, lymphocytic infiltrates in peripheral tissue, the presence of auto-reactive antibodies, and immune-complex-type glomerulonephritis, suggesting that PKC δ is important for the establishment of B-cell tolerance (Miyamoto *et al*, 2002). Adoptive transfer experiments suggest that the hyperproliferation phenotype observed in δ KO mice is B-cell autonomous. To further delineate specific aspects of autoimmune disease in the δ KO mice, we have focused on salivary gland pathology and function. Here, we report that δ KO mice display exocrine gland tissue injury and salivary gland dysfunction indicative of a SS-like autoimmune disease. This suggests that PKC δ is important for maintaining salivary gland homeostasis and perhaps for protecting salivary and other exocrine glands from immune-injury.

Materials and methods

Animals

δ KO mice on the C57Bl/6 background were a generous gift from Dr. K. Nakayama of Kyushu University, Fukuoka, Japan (Miyamoto *et al*, 2002). Wild-type C57BL/6 littermates were used as controls for all studies. Mice were bred and maintained under specific pathogen-free conditions in the Center for Comparative Medicine at University of Colorado Anschutz Medical Campus, which is an AAALAC-approved facility. The protocols used in this study were approved by the University of Colorado IACUC. Except as noted, only female mice, with ages ranging from 6 weeks to 12 months, were used for these studies.

Salivary flow rates

To stimulate salivation, mice were given an intraperitoneal injection of carbachol (Sigma, St Louis, MO, USA) dissolved in saline (0.25 mg kg⁻¹ of body weight) two min prior to measuring salivary flow rate. Saliva was collected for 5 min using a micropipette. Salivary flow rates are expressed as μ l min⁻¹.

Immunohistochemistry

Mice were anesthetized with Advertin, exsanguinated, and the submandibular glands (SMG) were removed and fixed in 10% formalin prior to embedding in paraffin. Hematoxylin and eosin (H&E)-stained sections were used for standard histological examination. For immunohistochemical staining, 4 μ M sections were deparaffi-

nized by heating at 60°C for 1 h and re-hydrated. Following antigen retrieval, endogenous peroxidases were quenched with 3% H₂O₂ and sections were blocked using Vectastain Elite ABC kit (Vector Laboratories PK-6100, Burlingame, CA, USA). Sections were incubated with anti-Ki-67 (1:50; Dako M7249, Carpinteria, CA, USA), anti-CD45R (1:100; BD Pharmigen 550286, San Jose, CA, USA), or anti-CD3 (1:100; Nova Castra NCL CD3-12, Buffalo Grove, IL, USA), or anti-IL-4 (1:100; Abcam, Cambridge, MA, USA), or anti-IFN- γ (1:50; R&D Systems, Minneapolis, MN, USA) for 1 h at room temperature, followed by incubation with secondary antibody (Vector Laboratories PK-6100) for 30 min at room temperature. Signal was detected with diaminobenzidine substrate (Sigma D6190) and counterstained with Gill's Hematoxylin (1:3; Vector Laboratories H-3401) or methyl green (Vector Laboratories H-3402).

Foci counting and scoring

Submandibular glands were removed and fixed in 10% formalin and paraffin embedded. Five 4 μ M sections were cut per animal, at least 50 μ M apart, and stained with H&E. Female mice 6–8 months old (WT, $n = 7$; δ KO, $n = 13$) or 12 months old (WT, $n = 7$; δ KO, $n = 6$) and 12-month-old male mice (WT, $n = 4$; δ KO, $n = 6$) were used in the study. The slides were blinded and evaluated by a pathologist for total number of foci of lymphocytic infiltrates and were graphed as number of foci/section. The same sections were subsequently scored a second time to access the degree of infiltration and tissue damage, and a score was assigned as previously described (White and Casarett, 1974). A focal score of 1 indicates that 1–5 foci of mononuclear cells were seen (more than 50 cells per focus) per section; 2 indicates that more than five foci of mononuclear cells were seen, but without significant parenchymal destruction; 3 indicates that multiple confluent foci were seen, with moderate degeneration of parenchymal tissue; 4 indicates extensive infiltration of the gland with mononuclear cells, and extensive parenchymal destruction.

Detection of anti-nuclear autoantibody (ANA)

Indirect immunofluorescence was performed using HEP-2 cell substrate slides according to the manufacturer's directions (INOVA, San Diego, CA, USA). Wild type and δ KO sera were diluted 1:100, and goat anti-mouse IgG-FITC antibodies were diluted 1:400. Slides were mounted using Vectashield Mounting Medium with 4',6-diamidino-2-phenylindole (VECTOR Laboratories). Fluorescence images were taken with Zeiss (Thornwood, NY, USA) Axiovert 200M microscope and a Zeiss AxioCam MRm camera using the 20 \times or 40 \times 0.75 NA objectives for evaluation. Color images were evaluated using Adobe Photoshop version 7.

Results

The SMGs of δ KO mice contain lymphocytic foci typical of SS

Lymphocytic infiltrates are most often detected in the SMGs in the animal models and present as focal,

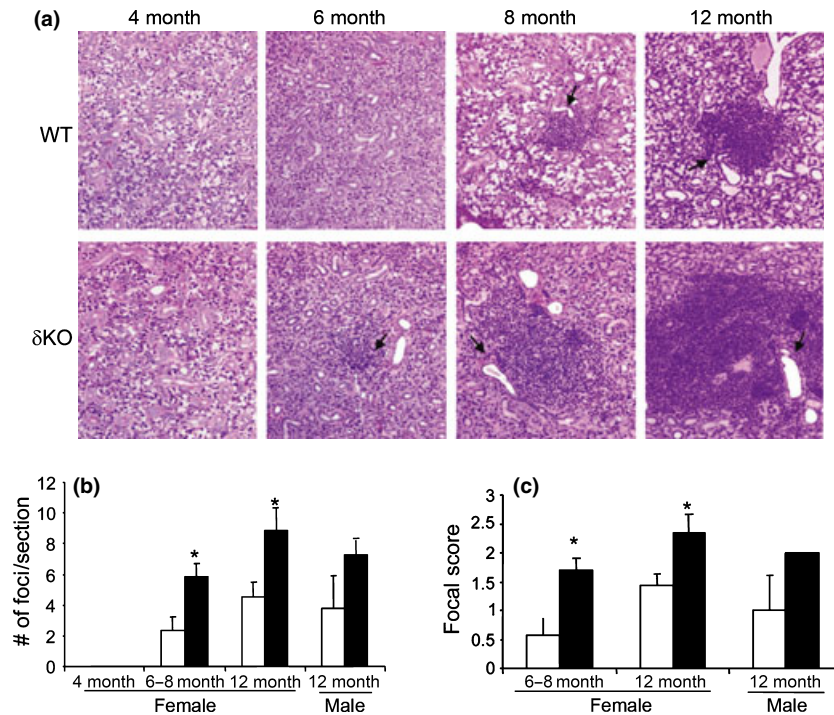


Figure 1 Lymphocytic infiltration in the submandibular glands (SMGs) of δ KO mice with age. (a) Pathology of SMGs from WT and δ KO mice. Four μ M sections of the SMGs from WT (top panel) and δ KO (bottom panel) female mice at 4, 8, and 12 months old were stained with H + E. Representative images at 200 \times are shown. Arrows indicate the location of interlobular ducts. (b) Quantification of lymphocytic infiltrates in the SMG. Graph shows a comparison of the foci number in the SMGs of female mice at 4 months, 6–8 months, and 12 months of age, and male mice at 12 months of age; WT = white bars and δ KO = black bars. The total number of foci in five 4 μ M sections per animal (50 μ M apart) was counted blindly, and the data are presented as average number of foci/section; * $P < 0.05$ compared with WT using a two-tailed *t*-test. (c) Graph shows scoring of lymphocytic foci in the SMGs of WT and δ KO female mice at 6–8 month (WT, $n = 7$; δ KO, $n = 13$) and 12 month of age (WT, $n = 7$; δ KO, $n = 6$), and in 12-month-old male mice (WT, $n = 4$; δ KO, $n = 6$); WT (white bars) and δ KO (black bars). Scoring was performed blindly by a pathologist using the White–Cassaret method (15). The average score of the five sections was used to determine the total focal score for the animal; * $P < 0.05$ compared with WT using a two-tailed *t*-test

periductal accumulations of mononuclear cells, with or without destruction of the parenchymal tissue (Greenspan *et al*, 1974). Examination of sections of stained SMGs from female δ KO and WT littermates showed that as the mice aged there was an increase in the number and size of lymphocytic foci; however, foci number and size were significantly increased in δ KO mice compared with WT mice of the same age (Figure 1a–c). Foci were not observed in either the WT or the δ KO mice at 6 weeks or 4 months of age (data not shown). Beginning at 6 months of age, small foci were observed in both WT and δ KO females and the number of foci increased with age (Figure 1b). Female δ KO mice had a significantly increased total number of foci compared with WT mice at both 6–8 months ($P < 0.05$) and 12 months ($P < 0.05$) of age (Figure 1b,c). In addition, the foci present in the δ KO mice were significantly larger in size ($P < 0.05$) (Figure 1a). δ KO male mice at 12 months of age also displayed more lymphocytic foci than control male mice of the same age ($P =$ need to find this out) were slightly less foci, and the foci present were smaller in size, when compared to their female δ KO counterparts (Figure 1b).

The focal score reflects the degree of infiltration and tissue damage present in the gland (White and Casa-

rett, 1974). As seen in Figure 1c, δ KO female mice had an increased focal score at 6–8 months and 12 months, compared with WT mice of the same age. In 12-month-old female δ KO mice, which had the highest focal score, there were vast areas of the gland replaced by the infiltrate, with some mice having a focal score of three based on multiple confluent foci with moderate parenchymal destruction. The foci appeared to form around or adjacent to the large interlobular ducts, starting at 6 months of age (Figure 1a, arrows). This is consistent with what is observed in human labial salivary gland biopsies (Greenspan *et al*, 1974), and some animal models of SS (Jonsson *et al*, 1987; Takada *et al*, 2004). The acini and ducts were extensively replaced by these infiltrates in the more severe foci; however, fibrosis and destruction of acini and ducts in the areas adjacent to the foci were not observed. Because there was no damage of acini in areas adjacent to the foci, the majority of the secretory tissue in the SMGs was intact. Histological examination of glands from 12-month-old mice indicated that male δ KO mice tended to have much smaller foci than observed in females δ KO animals (Figure 1a); all 12-month-old male δ KO mice had a focal score of two, while female mice typically displayed higher grade lesions (Figure 1c).

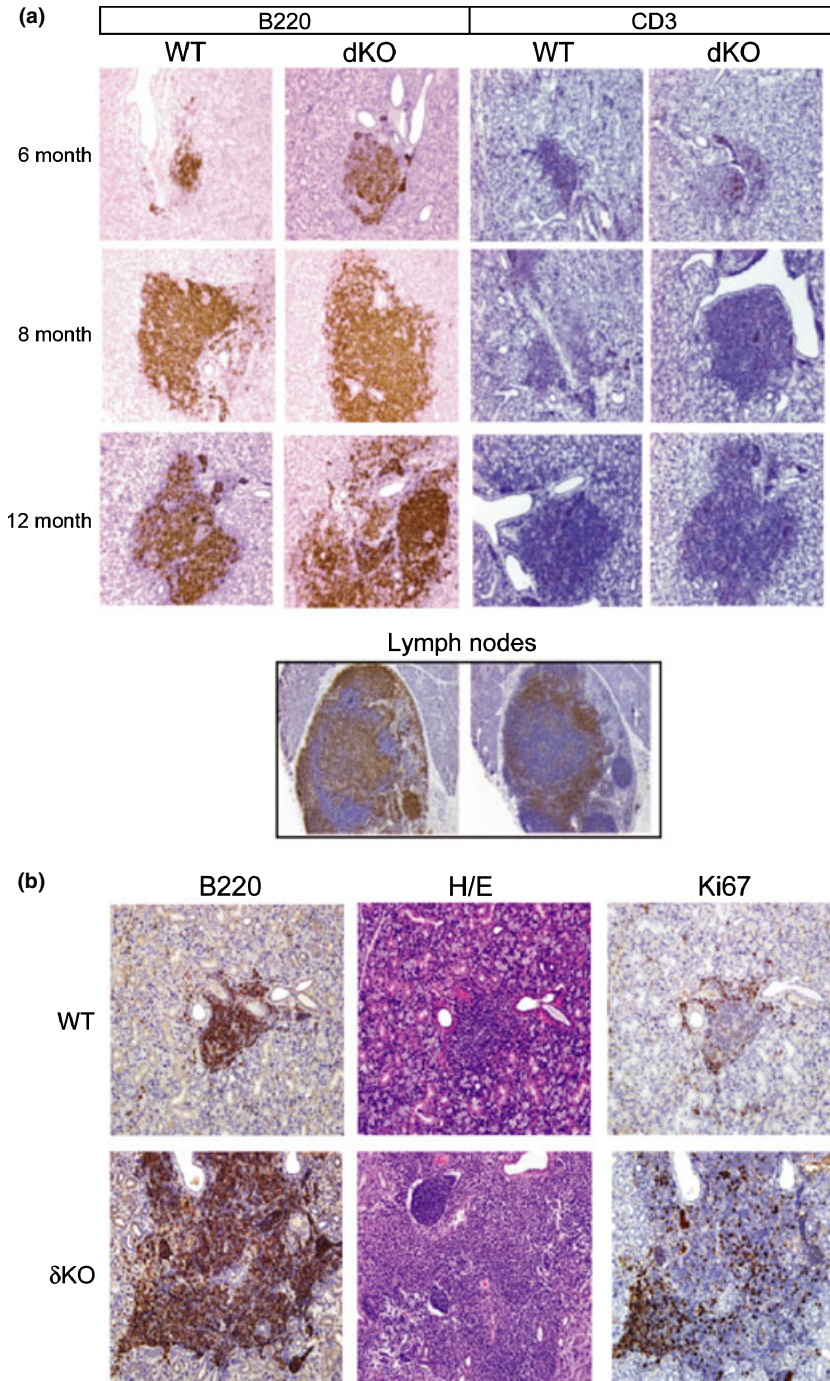


Figure 2 B220+ B cells are the predominant lymphocyte present in the foci. (a) Four μ M serial sections of the submandibular glands from WT and δ KO female mice at 6, 8, and 12 months old were stained with either anti-B220 (left panel) to stain B lymphocytes or anti-CD-3 (right panel) to stain T lymphocytes. Sections were counterstained with hematoxylin. Pictures were taken at 200 \times magnification. Lymph nodes (bottom panel) were used as positive controls for anti-B220 and anti-CD-3 antibodies. (b) Four μ M serial sections were taken from WT (top panel) or δ KO (bottom panel) female mice at 12 months of age and stained for anti-B220 (left panel), H + E (middle panel), and anti-Ki-67 (right panel). Pictures were taken at 200 \times magnification

B-cells predominate in the lymphocytic infiltrate in SMGs
To determine the subset of immune cells present in the infiltrates, immunohistochemistry was performed using anti-B220 to detect B cells and anti-CD3 to detect T cells (Figure 2a). Lymphocytic infiltrates in the SMGs of δ KO mice showed an intense staining for B220, suggesting that B cells represent the major infiltrating lymphocytes. No change in staining intensity was observed between the small, early foci, and the larger foci that appeared in older mice. The increase in peripheral B cells in the SMGs in δ KO mice is consistent with an increased expansion of B cells observed in these

mice (Mecklenbrauker *et al*, 2002; Miyamoto *et al*, 2002). Immunohistochemical staining with anti-CD3 antibody showed weak staining at all time points observed, suggesting a smaller population of T cells was present in the infiltrates (Figure 2a). No difference in the extent of anti-CD3 staining was observed between WT and δ KO mice, regardless of the age of the mice examined (Figure 2a).

Some human patients with autoimmune and/or other inflammatory diseases, including patients with SS, have infiltrates in non-lymphoid tissue that closely resemble organized lymphoid tissue with germinal centers (GCs)

(Stott *et al*, 1998; Salomonsson *et al*, 2003). These GC-like structures have dense populations of proliferating B cells, along with T cells and plasma cells. To determine whether the B220+ B cells present in the lymphocytic infiltrates in the SMG were proliferating, we stained serial sections with anti-B220 and Ki-67, a marker for proliferating cells. Ki-67 staining was observed in foci from both WT and δ KO SMGs, and the Ki-67 staining overlapped the B220 staining (Figure 2b). The intensity of Ki-67 staining correlated with the size of the foci; in small foci, there were considerably fewer cells that stained positive for Ki-67 (Figure 2b, top panel) than were observed in very large foci (Figure 2b, bottom panel). Interestingly, focus size and not the loss of PKC δ correlated with the number of proliferating cells in these lesions as large foci that were present in the glands of WT mice displayed strong Ki-67 staining (data not shown). The presence of proliferating B220+ B cells in the foci, and large amount of proliferating cells in these larger, more confluent foci, suggested that GC-like structures may be present in the SMGs of mice that have extensive lymphocytic infiltrates.

Salivary gland hypofunction in δ KO mice

To determine whether the δ KO mice display salivary hypofunction consistent with a SS-like disorder, saliva was collected after stimulation of salivation with carbachol. WT and δ KO female mice at 6 and 12 weeks of age exhibited similar salivary flow rates (Figure 3). At 4 months of age, however, the flow rate observed in δ KO mice was reduced by 35% compared with WT mice and was significantly reduced at all later time points examined (Figure 3). A trend toward decreased salivary flow rates was also observed in 10- and 12-month-old WT mice, compared with the flow rates observed in WT mice at four to 8 months of age. This may reflect the increased number of lymphocytic infiltrates observed in the SMGs of older WT mice; however, this decrease in salivary flow rate was not statistically significant. It is interesting to note that salivary gland hypofunction was detectable at 4 months of age in the δ KO mice, which proceeds the time at which lymphocytic infiltrates first appear in these mice (6 months of age; Figure 1a). This

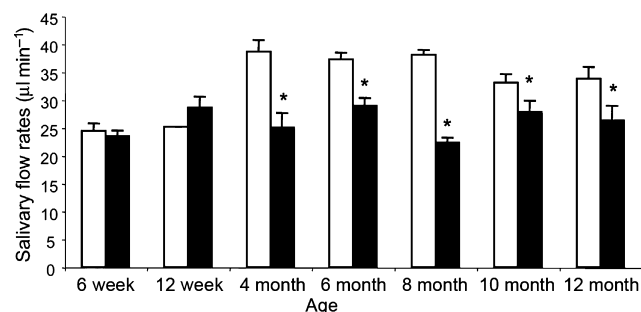


Figure 3 Salivary flow rates decrease with age in δ KO females. Saliva was collected for 5 min following injection of 0.25 mg kg⁻¹ of carbachol. Total saliva volume was measured using a pipette, and salivary flow rates are depicted as μ l of saliva/min of collection; WT = white bars, δ KO = black bars; * P < 0.5 compared with wild type, using a two-tailed t -test

differs from other SS animal models and human patients with SS in which the appearance of lymphocytic infiltrates occurs prior to, or concurrent with, salivary hypofunction (Jonsson *et al*, 2007). It should be noted that even though lymphocytic infiltrates were observed in WT control mice at later time points (Figure 1a) only the δ KO mice displayed statistically significant salivary hypofunction. The differences in salivary flow rates in WT and δ KO mice may be explained by the extent of lymphocytic infiltrates, which are more severe in δ KO mice, or perhaps differences in immunoglobulin subsets and/or the cytokines expressed in δ KO mice vs WT mice. The secretory dysfunction observed in these mice does not appear to correlate with extensive loss of secretory tissue, because the majority of the secretory tissue remains intact. Also, the secretory dysfunction was observed as early as 4 months, prior to the presence of lymphocytic infiltrates.

ANA are present in the serum of δ KO mice

Because autoantibodies that are specific for nuclear proteins, DNA or RNA molecules are commonly detected in rheumatic autoimmune diseases and serum samples from WT and δ KO mice were screened for the presence of ANA by staining of HEp-2 cells and evaluated for signal intensity and the pattern of staining by three independent evaluators. Figure 4 illustrates different patterns of staining that are indicative of ANA present in SS. None of the samples of mouse serum showed the diffuse staining pattern that is commonly observed in patients with either rheumatoid arthritis or systemic lupus erythematosus. It is important to mention the presence of ANA in serum is not a disease-specific marker because the serum of normal individuals can also be positive for ANA; however, the absence of ANA in serum from patients with one of these autoimmune diseases, including SS, is very rare. As indicated in Table 1, 100% of serum samples from δ KO mice were positive for ANA beginning at an early age, while of 12.5% of the serum samples from WT mice were positive for ANA at 6 weeks, although more WT mice became positive as they aged. At younger ages, both mouse strains showed a coarse speckled staining pattern. With aging, the staining pattern tended to become more diversified in both strains (Table 1).

Elevated pro-inflammatory IFN- γ expression in the salivary glands of δ KO mice

Previous studies have demonstrated the upregulation of Th1-driven cytokine mRNAs such as IFN- γ in the salivary glands from patients with SS, while in contrast, expression levels of IL-4 mRNA are either absent, or slightly upregulated (Fox *et al*, 1994; Ohshima *et al*, 1996). Therefore, we examined the protein levels of IFN- γ and IL-4 in salivary glands from 8-month-old WT and δ KO mice by immunohistochemistry (Figure 5). Interestingly, IL-4 expression was slightly upregulated in the SMG from δ KO mice compared with WT mice, while IFN- γ expression was strongly upregulated in the SMG from δ KO mice compared with WT mice. This pattern is similar to that observed in SS, suggesting

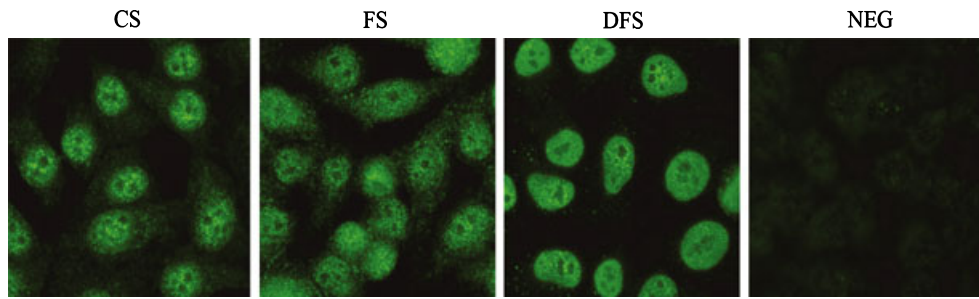


Figure 4 Examples of anti-nuclear autoantibody speckled nuclear staining patterns detected in δ KO sera. Hep-2 slides were incubated with WT and δ KO sera diluted 1:100 followed by anti-mouse IgG conjugated to FITC (green). Examples of nuclear coarse speckled (CS), fine speckled (FS), dense fine speckled (DFS), and negative (NEG) staining patterns as detected in δ KO sera are shown. A rating of the intensity of staining (1 through 3) was also assigned based on signal intensity by three different evaluators (Table 1)

that these cytokines may contribute to the progression of disease in the δ KO mouse model.

Discussion

Recent studies have suggested a crucial role of B cells and other lymphoid cells (Youinou *et al*, 2007) in various mouse models of SS, as well as in humans. Mice deficient for δ KO develop systemic autoimmune disease; however, salivary gland injury and function have not been studied in this model (Miyamoto *et al*, 2002). Here, we report that δ KO mice have several important and clinical features of human SS (Soyfoou *et al*, 2007).

Histopathological examination of the SMGs of δ KO female mice revealed the presence of focal and interlobular infiltrates beginning at 6 months of age, which increased in both number and intensity with age (Figure 1). Many of the larger foci had replaced extensive areas of acini and ducts with lymphocytes; however, no damage was observed in adjacent acini and ducts. The presence of infiltrates in the SMGs of the WT mice is consistent with previous reports, in which infiltrates were observed starting at 6 months of age because of age-related breakdown of tolerance (Hayashi *et al*, 1989).

However, δ KO mice displayed an increased number and intensity of infiltrates at all time points measured compared with WT mice (Figure 1). δ KO male mice at 12 months of age had fewer and less intense infiltrates than the same structures observed in female mice, although the differences observed did not reach statistical significance. Although not addressed here, it is possible that loss of PKC δ may accelerate the breakdown in tolerance associated with aging in the C57Bl/6 mice.

Immunohistochemical analysis of the infiltrates revealed that the predominant lymphocyte present in the foci was B220+ B cells, with a smaller amount of CD3+ T cells interspersed throughout the foci (Figure 2b). The increase in peripheral B cells in the SMGs of δ KO mice is consistent with an increased expansion of B cells reported in these mice (Mecklenbrauker *et al*, 2002; Miyamoto *et al*, 2002). The predominance of B cells in the lymphocytic infiltrates observed in the δ KO mice differ from that observed in human patients with SS, in which CD4+ and CD8+ T cells are predominant in the infiltrates, at least during the early stage of the disease (1). However, the B-cell hyperactivity observed in δ KO mice is consistent with that which has been observed in many human patients with SS (Fox and Kang, 1992; Hansen *et al*, 2002, 2005).

Table 1 Distribution of ANA staining patterns in PKC δ WT and KO mice

Pattern	Intensity	6 weeks		4 months		8 months		12 months	
		WT (8)	KO (2)	WT (4)	KO (4)	WT (0)	KO (5)	WT (9)	KO (6)
		# Mice	# Mice	# Mice	# Mice	# Mice	# Mice	# Mice	# Mice
CS	1	1	1	1	1	0	1	0	1
	2	0	1	0	3	0	0	1	2
	3	0	0	1	0	0	1	1	1
FS	1	0	0	0	0	0	0	0	0
	2	0	0	0	0	0	1	2	1
	3	0	0	0	0	0	0	1	1
DFS	1	0	0	0	0	0	0	0	0
	2	0	0	0	0	0	1	0	0
	3	0	0	0	0	0	1	4	0
NEG	NA	7	0	2	0	0	0	0	0
% Positive		12.5	100	50	100	NA	100	100	100

Numbers in parenthesis indicate mouse number for screening. Intensity graded from 1 to 3 with 1 being weakest and 3 being strongest in expression. CS, coarse speckled; FS, fine speckled; DFS, dense fine speckled; NEG, negative; WT, wild-type mice; KO, PKC δ -/- mice.

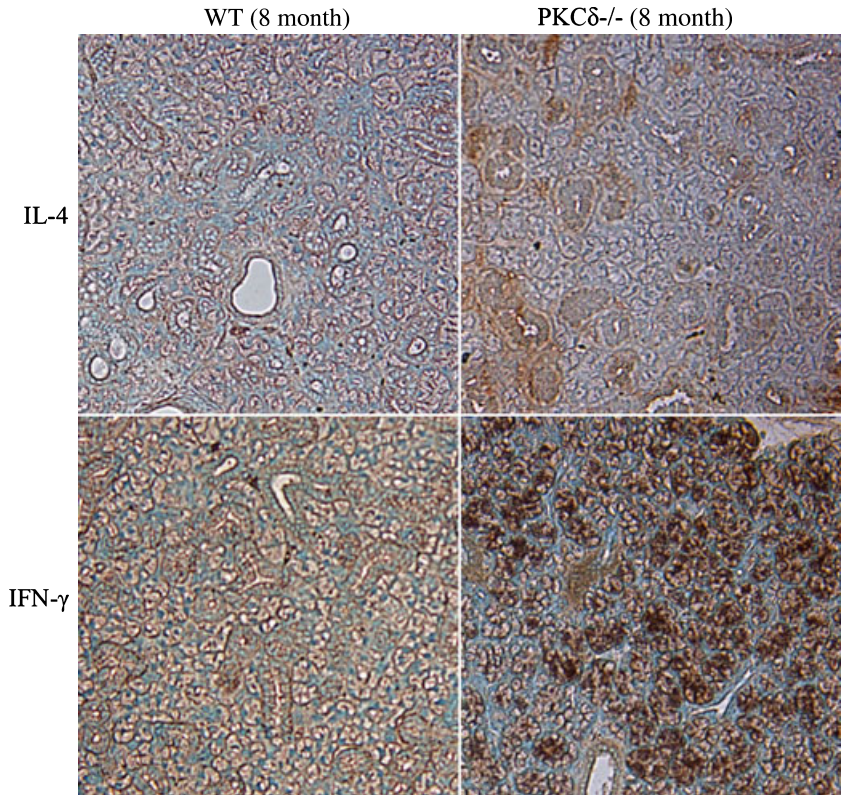


Figure 5 Upregulated IFN- γ expression in salivary glands of PKC δ ^{-/-} mice. IL-4 and IFN- γ expression in salivary gland sections from 8-month-old WT and δ KO mice was examined by immunohistochemistry. IL-4 expression was slightly upregulated in δ KO mice, while IFN- γ expression was greatly upregulated in δ KO mice (brown)

δ KO mice display many of the characteristics of BAFF transgenic mice, such as lymphocytic infiltrates consisting largely of B220⁺ cells, salivary hypofunction, and increased production of immunoglobulins and autoantibodies (Groom *et al*, 2002). BAFF has been shown to promote B-cell survival by inhibiting nuclear accumulation of PKC δ ; nuclear accumulation of PKC δ is essential to its ability to induce apoptosis (Mecklenbrauker *et al*, 2004) (DeVries *et al*, 2002). δ KO B cells do not die upon BAFF withdrawal; however reconstitution with a constitutively nuclear form of PKC δ restores BAFF sensitivity; suggesting that PKC δ is the critical downstream target of BAFF signaling (Mecklenbrauker *et al*, 2004). Consistent with this scenario, enhanced proliferation and survival of B cells and the presence of GCs in unstimulated lymphoid tissue have been reported in δ KO mice (Miyamoto *et al*, 2002). Structures resembling GCs are likewise seen in the salivary glands of patients with SS (Stott *et al*, 1998). The presence of Ki-67-staining B220⁺ cells also suggests the presence of germinal cell-like structures in the salivary glands of δ KO mice (Figure 2).

A critical aspect of SS, which is surprisingly missing from many models, is loss of secretory function (Soyfoo *et al*, 2007). Analysis of salivary flow rates of the δ KO mice revealed a reduction in salivary flow rates which began at 4 months and preceded inflammation of SMGs (Figure 3). Although WT mice exhibited infiltration of lymphocytes into their SMGs, they did not display salivary hypofunction to the extent observed in the δ KO mice. Interestingly, although there are reports that

C57BL/6 mice sometimes develop autoimmunity as they age (25), this autoimmune reaction is clearly distinct from the autoimmunity we observe in δ KO mice as salivary gland function was not affected in the C57BL/6 mice (Figure 3), and IFN- γ was not significantly upregulated in the salivary glands (Figure 5). These characteristics are known to distinguish SS-like disease from other inflammatory conditions.

Previous reports have also shown that δ KO mice have hypergammaglobulinemia, characterized particularly by the increased expression of IgG1 and IgA at 6 months of age and older (Miyamoto *et al*, 2002). In addition, autoantibodies such as anti-chromatin and ANA have been described in the sera of δ KO mice as they age, although there are conflicting reports with regard to the presence of ANA as well as elevated serum levels of IL-6 (Mecklenbrauker *et al*, 2002; Miyamoto *et al*, 2002). Unlike previous studies, we show that sera from δ KO mice contain ANA starting at 6 weeks of age, and we describe distinct nuclear staining patterns of ANA, which are commonly seen in autoimmune SS. All sera from δ KO mice were positive regardless of age; in contrast, only 1/7 control mice produced ANA at 6 weeks, 50% of the serum samples from WT mice was positive for ANA at 8 months, and all control serum samples were positive by 12 months of age (Table 1). This clearly indicates that auto-reactive B cells in δ KO mice may be due to failure of tolerance induction to nuclear antigens. In contrast, WT C57BL/6 mice tend to lose tolerance to self-antigens over time, which is an indicative of age-induced breakdown of tolerance. The overall staining patterns tend to diversify

as both groups of mice get older, potentially implying diversification of B-cell repertoire engaging epitope spreading as the inflammation progresses.

Taken together, an inflammatory phenotype, indicated by lymphocytic infiltration, ANA production, and pro-inflammatory cytokine expression in the salivary glands, along with secretory dysfunction, which are clinical hallmarks of SS, was observed in the δ KO mouse model. In most animal models of SS, inflammation precedes secretory dysfunction, even if the level of inflammation does not always correlate with the degree of glandular hypofunction (Jonsson *et al*, 2007). In human patients', histological manifestations can likewise be variable from a complete absence of infiltrates to monoclonal B-cell expansion followed by the development of B-cell lymphoma. Our model resembles human SS based on focal infiltration, loss of secretion, and autoantibody production and maybe more reflective of human patients with GCs in the salivary glands, which is only 17% of the patient population (Kroneld *et al*, 1997; Hansen *et al*, 2002; Youinou *et al*, 2007). Finally, our model showing secretory dysfunction prior to immune cell infiltration supports the roles of soluble factors such as autoantibodies, cytokines, and/or nitric oxide in functional suppression of fluid secretion and/or altering structural integrity of the salivary glands in SS (Cha *et al*, 2006) (Baker *et al*, 2008; Caulfield *et al*, 2009). Taken together, our data support the conclusion that δ KO mice have exocrine gland tissue damage indicative of a SS-like phenotype.

Acknowledgements

This work was supported by Public Health Service grants DE015648 (MER), DE019644 (SHC), and DE016354 (SMA).

Author contributions

GPB, KMP, BAP, CJC, MO, designed and executed experiments, participated in data analysis; GPB, MSS, SC, SMA, MER, experimental design, data analysis and manuscript preparation.

References

Allen-Petersen BL, Miller MR, Neville MC *et al* (2010). Loss of protein kinase C delta alters mammary gland development and apoptosis. *Cell Death Dis* **1**: e17.
 Baker OJ, Camden JM, Redman RS *et al* (2008). Proinflammatory cytokines tumor necrosis factor-alpha and interferon-gamma alter tight junction structure and function in the rat parotid gland Par-C10 cell line. *Am J Physiol Cell Physiol* **295**: C1191–C1201.
 Bowman SJ, Ibrahim GH, Holmes G, Hamburger J, Ainsworth JR (2004). Estimating the prevalence among Caucasian women of primary Sjogren's syndrome in two general practices in Birmingham, UK. *Scand J Rheumatol* **33**: 39–43.
 Caulfield VL, Balmer C, Dawson LJ, Smith PM (2009). A role for nitric oxide-mediated glandular hypofunction in a non-apoptotic model for Sjogren's syndrome. *Rheumatology (Oxford)* **48**: 727–733.

Cha S, Singson E, Cornelius J, Yagna JP, Knot HJ, Peck AB (2006). Muscarinic acetylcholine type-3 receptor desensitization due to chronic exposure to Sjogren's syndrome-associated autoantibodies. *J Rheumatol* **33**: 296–306.
 Devauchelle-Pensec V, Penne Y, Morvan J *et al* (2007). Improvement of Sjogren's syndrome after two infusions of rituximab (anti-CD20). *Arthritis Rheum* **57**: 310–317.
 DeVries TA, Neville MC, Reyland ME (2002). Nuclear import of PKCdelta is required for apoptosis: identification of a novel nuclear import sequence. *EMBO J* **21**: 6050–6060.
 Fox RI, Kang HI (1992). Pathogenesis of Sjogren's syndrome. *Rheum Dis Clin North Am* **18**: 517–538.
 Fox RI, Kang HI, Ando D, Abrams J, Pisa E (1994). Cytokine mRNA expression in salivary gland biopsies of Sjogren's syndrome. *J Immunol* **152**: 5532–5539.
 Greenspan JS, Daniels TE, Talal N, Sylvester RA (1974). The histopathology of Sjogren's syndrome in labial salivary gland biopsies. *Oral Surg Oral Med Oral Pathol* **37**: 217–229.
 Groom J, Kalled SL, Cutler AH *et al* (2002). Association of BAFF/BLyS overexpression and altered B cell differentiation with Sjogren's syndrome. *J Clin Invest* **109**: 59–68.
 Hansen A, Odendahl M, Reiter K *et al* (2002). Diminished peripheral blood memory B cells and accumulation of memory B cells in the salivary glands of patients with Sjogren's syndrome. *Arthritis Rheum* **46**: 2160–2171.
 Hansen A, Reiter K, Ziprian T *et al* (2005). Dysregulation of chemokine receptor expression and function by B cells of patients with primary Sjogren's syndrome. *Arthritis Rheum* **52**: 2109–2119.
 Hayashi Y, Utsuyama M, Kurashima C, Hirokawa K (1989). Spontaneous development of organ-specific autoimmune lesions in aged C57BL/6 mice. *Clin Exp Immunol* **78**: 120–126.
 Humphreys-Beher MG, Brayer J, Yamachika S, Peck AB, Jonsson R (1999). An alternative perspective to the immune response in autoimmune exocrinopathy: induction of functional quiescence rather than destructive autoaggression. *Scand J Immunol* **49**: 7–10.
 Humphries MJ, Limesand KH, Schneider JC *et al* (2006). Suppression of apoptosis in the protein kinase C delta null mouse in vivo. *J Biol Chem* **281**: 9728–9737.
 Jonsson R, Tarkowski A, Backman K, Holmdahl R, Klare-skog L (1987). Sialadenitis in the MRL-l mouse: morphological and immunohistochemical characterization of resident and infiltrating cells. *Immunology* **60**: 611–616.
 Jonsson MV, Delaleu N, Jonsson R (2007). Animal models of Sjogren's syndrome. *Clin Rev Allergy Immunol* **32**: 215–224.
 Khare SD, Sarosi I, Xia XZ *et al* (2000). Severe B cell hyperplasia and autoimmune disease in TALL-1 transgenic mice. *Proc Natl Acad Sci U S A* **97**: 3370–3375.
 Kroneld U, Halse AK, Jonsson R, Bremell T, Tarkowski A, Carlsten H (1997). Differential immunological aberrations in patients with primary and secondary Sjogren's syndrome. *Scand J Immunol* **45**: 698–705.
 Mecklenbrauker I, Saijo K, Zheng NY, Leitges M, Tarakhovskiy A (2002). Protein kinase Cdelta controls self-antigen-induced B-cell tolerance. *Nature* **416**: 860–865.
 Mecklenbrauker I, Kalled SL, Leitges M, Mackay F, Tarakhovskiy A (2004). Regulation of B-cell survival by BAFF-dependent PKCdelta-mediated nuclear signalling. *Nature* **431**: 456–461.
 Miyamoto A, Nakayama K, Imaki H *et al* (2002). Increased proliferation of B cells and auto-immunity in mice lacking protein kinase Cdelta. *Nature* **416**: 865–869.

- Nishizuka Y (1992). Intracellular signaling by hydrolysis of phospholipids and activation of protein kinase C. *Science* **258**: 607–614.
- Ohyama Y, Nakamura S, Matsuzaki G et al (1996). Cytokine messenger RNA expression in the labial salivary glands of patients with Sjogren's syndrome. *Arthritis Rheum* **39**: 1376–1384.
- Reyland ME (2009). Protein kinase C isoforms: multi-functional regulators of cell life and death. *Front Biosci* **14**: 2386–2399.
- Salomonsson S, Jonsson MV, Skarstein K et al (2003). Cellular basis of ectopic germinal center formation and autoantibody production in the target organ of patients with Sjogren's syndrome. *Arthritis Rheum* **48**: 3187–3201.
- Soyfoo MS, Steinfeld S, Delporte C (2007). Usefulness of mouse models to study the pathogenesis of Sjogren's syndrome. *Oral Dis* **13**: 366–375.
- Stott DI, Hiepe F, Hummel M, Steinhauser G, Berek C (1998). Antigen-driven clonal proliferation of B cells within the target tissue of an autoimmune disease. The salivary glands of patients with Sjogren's syndrome. *J Clin Invest* **102**: 938–946.
- Takada K, Takiguchi M, Konno A, Inaba M (2004). Spontaneous development of multiple glandular and extraglandular lesions in aged IQ1/Jic mice: a model for primary Sjogren's syndrome. *Rheumatology (Oxford)* **43**: 858–862.
- Ware CF (2000). APRIL and BAFF connect autoimmunity and cancer. *J Exp Med* **192**: F35–F38.
- White SC, Casarett GW (1974). Induction of experimental autoallergic sialadenitis. *J Immunol* **112**: 178–185.
- Youinou P, Devauchelle V, Hutin P, Le Berre R, Saraux A, Pers JO (2007). A conspicuous role for B cells in Sjogren's syndrome. *Clin Rev Allergy Immunol* **32**: 231–237.

Copyright of Oral Diseases is the property of Wiley-Blackwell and its content may not be copied or emailed to multiple sites or posted to a listserv without the copyright holder's express written permission. However, users may print, download, or email articles for individual use.